Tutor/s

Dr. Jordi Bonet Ruiz
Department of Chemical Engineering

Dr. Joan Llorens Llacuna
Department of Chemical Engineering

Grau en Enginyeria Química

Treball Final de Grau

Fluid circulation simulation in heat exchangers: Shell and tube (CFD - ANSYS®)

Simulació de la circulació de fluids en bescanviadors de calor: Carcassa i tubs (CFD - ANSYS®)

Gerard Minella Sivill

June 2016

UNIVERSITAT DE BARCELONA

Si no conozco alguna cosa, la investigaré

Louis Pasteur

En primer lloc voldria donar les gràcies als meus tutors per tota la dedicació, paciència i confiança que m'han mostrat durant aquests mesos. A part de ser grans professors sou grans persones.

Als companys amb qui durant aquests anys de carrera hem anat fent camí i les grans hores de feina conjunta per a tirar endavant. Sobretot fer menció als companys que han cursat aquest semestre el TFG amb qui més relació he tingut durant aquest temps i he pogut conèixer amb més detall.

A la meva parella, que sempre m'ha sabut animar en els mals moments i per tota la paciència que ha tingut amb mi, gràcies pel dia a dia, ets un dels pilars fonamentals de la meva vida.

Als meus pares, que són les persones que m'han fet créixer i ser com sóc, estic molt orgullós de tot el que han fet per mi, gràcies.

Al meu avi, el Nonno, sense tu no hagués arribat pas on sóc, les infinites gràcies de tot cor per tot el que has fet per mi, hi ha coses que no s'oblidaran mai a la vida i a tu et portaré eternament dins del meu cor. "*Siempre sucede lo mejor*" que tu dius.

REPORT

CONTENTS

1. SUMMARY

In this final project degree several simulations are performed on shell and tube heat exchanger using ANSYS® v16.2 software - student version.

This software contains the simulation tool Fluent which is specific to Computational Fluid Dynamics (CFD) applications, which allows the resolution of the mathematical model at microscopic level.

This software is used to generate the geometry of the heat exchanger and mesh. Boundary conditions and turbulence model are selected according to the recommended or generally used for this particular issue.

ANSYS® results are compared to the classical equations available in chemical engineering handbooks. A rather good agreement is obtained and the main differences are consequence of the fact that in classical equations it is assumed that the profiles are stabilized meanwhile in the simulations are not.

Keywords: Convection coefficient, Pressure drop, Turbulence, Mesh, Microscopic Balance.

2. RESUM

En el present treball final de grau, es duen a terme vàries simulacions d'un bescanviador de calor de carcassa i tubs mitjançant el software ANSYS® v16.2 versió d'estudiant.

Aquest software conté l'eina de simulació Fluent que és específica per l'aplicació en dinàmica de fluids computacional (CFD), que permet resoldre els models matemàtics a nivell microscòpic.

El software s'utilitza per generar la geometria del bescanviador de calor amb el seu mallat corresponent. Les condicions de contorn i el model de turbulència són seleccionats d'acord amb el que es recomana o s'utilitza generalment per aquest estudi en particular.

Els resultats d'ANSYS® són comparats amb les equacions clàssiques disponibles en els handbooks d'enginyeria química. Les principals diferències resulten ser conseqüència del fet que en les equacions clàssiques s'assumeix que els perfils estan estabilitzats mentre que en les simulacions no.

Paraules clau: Coeficient de convecció, Pèrdues de càrrega, Turbulència, Mallat, Balanços microscòpics.

3. INTRODUCTION

Shell and tube heat exchangers in their various forms are probably the most widespread and commonly used equipment in the process industries. They are essential equipment for all the major industries like chemical and petrochemical plants, oil refineries, power plants and metallurgical operations. They are employed for several applications such as heating, cooling, condensation and boiling.

Shell and tube consists of a bundle of tubes enclosed in a cylindrical shell. Shell baffles direct the fluid flow and support the tubes. The basic principle of a heat exchangers is two fluids flowing at different temperatures separated by a wall. The driving force for heat transfer by conduction and convection is the temperature difference at both sides of the wall.

During the past 25 years, Computational Fluid Dynamics (CFD) is being increasingly used due to the increase of computational power as well as numerical techniques. Novel baffles configurations and shapes have been developed in order to improve heat transfer efficiency and low pressure drops. The presence of baffles produce complex flow patterns not covered in classical chemical engineering equations and CFD has been used for their assessment. Trefoil-hole baffles (Zhou et al, 2015) and ROD-baffles (Dong et al, 2007) are studied as alternative to common baffles. On the other hand, on the tube side, helically coiled tube (Alimoradi and Veysi, 2016) has been evaluated.

Figure 1. Typical shell and tube heat exchanger

3.1. SHELL AND TUBE CLASSICAL MODEL

The classical equations for shell and tubes to determine the convection coefficient h and the pressure drop ΔP for turbulent flow are presented in this section. The shell-side convection coefficient (Eq. 1) and pressure drop (Eq. 2) are calculated using the expressions indicated by Sinnott (2008). The tubes-side convection coefficient (Eq. 3) and pressure drop (Eq. 4) are calculated using the expressions indicated by Levenspiel (1993) and Sinnott (2008) respectively. The equation 3 has been taken from Levenspiel (1993) instead of the Sinnott (2008) expression because it includes a correction term considering the ratio of equivalent diameter and length that makes it more accurate.

$$Nu = \frac{h_s\, d_e}{k_f} = j_h\, Re\, Pr^{1/3} \left(\frac{\mu}{\mu_w}\right)^{0.14} \tag{1}$$

$$\Delta P_s = 8\, j_f \left(\frac{D_s}{d_e}\right) \left(\frac{L}{l_B}\right) \frac{\rho\, u_s^2}{2} \left(\frac{\mu}{\mu_w}\right)^{-0.14} \tag{2}$$

$$Nu = \frac{h_i\, d_e}{k} = 0.023 \left[1 + \left(\frac{d_e}{L}\right)\right]^{0.7} Re^{0.8}\, Pr^{1/3} \left(\frac{\mu}{\mu_w}\right)^{0.14} \tag{3}$$

$$\Delta P_i = 8\, j_f \left(\frac{L}{d_i}\right) \rho \frac{u^2}{2} \left(\frac{\mu}{\mu_w}\right)^{-0.14} \tag{4}$$

3.2. COMPUTATIONAL FLUID DYNAMICS (CFD) MODEL

Computational Fluid Dynamics is the name given to the numerical method of solving the mass (Eq 5) and energy (Eq 6) balances (continuity) and momentum equations (Eq 7 and 8) (all of them are called transport equations) including also other equations such as turbulence equations. The following transport equations are in the form in which they are implemented in ANSYS® Fluent 16.2 student-version. Its solver solves the 3D Cartesian coordinate, finite volume transient transport equations.

The equation for conservation of mass, or continuity equation, can be written as follows:

$$\frac{\partial \rho}{\partial t} + \nabla \cdot (\rho\, \vec{u}) = 0 \tag{5}$$

The conservation of energy is described by:

$$\frac{\partial (\rho\, E)}{\partial t} + \nabla \cdot \left(\overrightarrow{u}(\rho\, E + P)\right) = -\nabla \cdot \left(\sum_j h_j J_j\right) + S \tag{6}$$

The conservation of momentum is described by:

$$\frac{\partial (\rho\, \vec{u})}{\partial t} + \nabla \cdot (\rho\, \vec{u}\, \vec{u}) = -\nabla P + \rho\, \vec{g} + \nabla \cdot (\overline{\overline{\tau}}) + \vec{F} \tag{7}$$

Where the stress tensor is given by:

$$\bar{\bar{\tau}} = \mu \left((\nabla \vec{u} + \nabla \vec{u}^r) - \frac{2}{3} \nabla \cdot \vec{u} I \right) \tag{8}$$

3.2.1. Turbulence Model

Turbulence is the three-dimensional unsteady random motion observed in fluids at moderate to high Reynolds numbers. Many quantities of technical interest depend on turbulence, including the mixing of momentum, energy and species, the heat transfer, the pressure losses and efficiency and the forces on aerodynamic bodies. It is considered turbulent flow when Re > 4,000 and fully turbulent flow when Re > 10,000.

3.2.1.1. Standard k-ε Model

Two-equation turbulence models allow the determination of both, a turbulent length and time scale by solving two separate transport equations. The standard *k-ε* model in ANSYS® Fluent falls within this class of models and has become the workhorse of practical engineering flow calculations. Robustness, economy, and reasonable accuracy for a wide range of turbulent flows explain its popularity in industrial flow and heat transfer simulations. It is a semi-empirical model, and the derivation of the model equations relies on phenomenological considerations and empiricism.

The standard *k-ε* model is based on model transport equations for the turbulence kinetic energy (*k*) and its dissipation rate (*ε*). The model transport equation for *k* is derived from the exact equation, while the model transport equation for *ε* was obtained using physical reasoning and bears little resemblance to its mathematically exact counterpart.

The standard *k-ε* model gets good prediction results at high Reynolds in a relatively simple geometry and works better than other models. Standard *k-ε* is also good at capturing the temperature profile. It is also observed that the standard *k-ε* model tends to overestimate the convection coefficient slightly (Pal et al, 2016).

3.2.1.2. Transport equations for the Standard k-ε Model

The turbulence kinetic energy, *k*, and its rate of dissipation, *ε*, are obtained from the following transport equations:

$$\frac{\partial k}{\partial t} + \frac{\partial (u_j) k}{\partial x_j} = \frac{1}{\rho} \frac{\partial}{\partial x_j} \left[\left(\mu + \frac{\mu_t}{\sigma_k} \right) \frac{\partial k}{\partial x_j} \right] + \frac{P_k}{\rho} - \varepsilon \qquad (9)$$

$$\frac{\partial \varepsilon}{\partial t} + \frac{\partial (u_j)\varepsilon}{\partial x_j} = \frac{1}{\rho}\frac{\partial}{\partial x_j}\left[\left(\mu + \frac{\mu_t}{\sigma_\varepsilon}\right)\frac{\partial \varepsilon}{\partial x_j}\right] + C_{\varepsilon 1}\frac{\varepsilon}{k}\frac{P_k}{\rho} - C_{\varepsilon 2}\frac{\varepsilon^2}{k} \quad (10)$$

Where:

$$P_k = \mu_t \left(\frac{\partial (u_i)}{\partial x_j} + \frac{\partial (u_j)}{\partial x_i}\right)\frac{\partial (u_i)}{\partial x_j}$$

The turbulent viscosity, μ_t, is computed by combining *k* and *ε* as follows:

$$\mu_t = \rho\, C_\mu \frac{k^2}{\varepsilon}$$

The model constants have the following default values:

$C_{1\varepsilon} = 1.44$; $C_{2\varepsilon} = 1.92$; $C_\mu = 0.09$; $\sigma_k = 1.0$; $\sigma_\varepsilon = 1.3$

These default values have been determined from experiments for fundamental turbulent flows.

3.3. ANSYS®

Industry leaders use ANSYS® to create complete virtual prototypes of complex products and systems, comprised of mechanical, electronics, fluids and embedded software components which incorporate all the physical phenomena that exist in real world environments (ANSYS®, 2016).

The general workflow of the CFD for ANSYS® modeling involves 5 major steps:

- Definition of the geometry
- Creation of the mesh from the model's geometry
- Establish the boundary conditions
- Solver
- Results visualization and treatment

3.3.1. Geometry (DesignModeler)

DesignModeler is the build in CAD (Computer Aided Drawing) package within the ANSYS® Fluent workbench project. Although external CAD files can be imported, it is preferable to use the built-in CAD for a better compatibility with the successive steps. The CAD sketch is the first step in the simulation process. Geometric forms represent actual design details or be an approximation of the design using simplified components.

3.3.2. Meshing

In order to analyze fluid flows, flow domains are split into smaller subdomains (made up of geometric primitives like hexahedral and tetrahedral in 3D), and discretized governing equations are solved inside each of these portions of the domain. Each of these portions of the domain are known as elements or cells, and the collection of all elements is known as mesh or grid. The continuous system of equations previously described is discretized in this work as finite elements defined by the mesh.

For the next step of this project, creating the mesh, the geometry previously created is imported to the Meshing module. Mesh generation is one of the most critical aspects of engineering simulation. The mesh controls must be set before meshing the solid model. Mesh controls allows to establish such factors as the element shape, midsize node placement, and element size to be used in meshing the sketch. Too many cells consume a lot of memory and it takes a longer time to solve the equations, and too few may lead to inaccurate results. Moreover, in the student version there are a limited number of nodes. Consequently an optimum mesh must be found (ANSYS® Meshing, 2016).

3.3.3. Boundary Conditions

ANSYS® Fluent sets the boundary and cell zone conditions in the current model by comparing the zone name associated with each set of conditions in the file with the zone names in the model. If the model does not contain a matching zone name for a set of boundary conditions, those conditions are ignored. Boundary conditions consist of flow inlets and outlets boundaries with its corresponding temperature, wall specifications, the symmetries, the pole boundaries and internal face boundaries.

3.3.4. Solver

The CFD defined equations are solved using an iterative numerical convergence method. This means criteria for stopping the process are needed. The choice of criteria depends on the CFD model used and requires some judgment by the user. ANSYS® Fluent produces residuals as indicators of convergence. Residuals are the differences in the value of a quantity between two iterations. This means that lower residuals then results less change. Furthermore, small residuals are a sign of mathematical convergence.

ANSYS® Fluent, by default, considers that the system converges when the values are under:

- 10^{-3} for the continuity equation.
- 10^{-3} for the x-velocity.
- 10^{-3} for the y-velocity .
- 10^{-3} for the z-velocity.
- 10^{-6} for the energy equation.
- 10^{-3} for the *k* equation.
- 10^{-3} for the ε equation.

3.3.5. Results

It is possible to export the results from the Solver into the visualitzation environment for an easy understanding using the Post program.

Several variables such as temperature, velocity, pressure, a.s.o. can be represented in different cut planes. Furthermore, the Post processing allows for instance the determination of variables such as the termometer temperature of tube section and the averaged convection coefficient. CFD-Post can generate isosurface, animations, particle tracks, streamlines, vector plots, countour plots, etc. providing an insight on the unit behaviour.

4. OBJECTIVES

The main objectives for this project are the following:

- Learn how to use properly the simulation software ANSYS® v16.2 student-version which was exposed in the subject Transport Phenomena of the Chemical Engineering degree of the University of Barcelona.

- Elaborate the geometry and the mesh of the problem in 3D, establish the boundary conditions and do some simulations with Fluent tool for Computational Fluid Dynamics, CFD.

- Obtain convection coefficients and pressure drop for co-current and counter-current cases in shell and tube heat exchangers simulated with ANSYS®.

- Compare convection coefficient and pressure drop simulated with ANSYS® with the ones obtained with analytical equations from the classical chemical engineering books.

- Plot the evolution of temperature, pressure and velocity in the simulations performed.

5. MATERIAL AND METHODS

This section consists of the description of the procedure used to perform the shell and tube heat exchanger simulation.

The heat exchanger operates either co-currently or counter-currently. It consists of a heat exchanger in 3D of 7 tubes, one in the middle and six equally distributed around the central tube and the shell. Two heat exchangers lengths are considered in this study: 0.2 m and 0.4 m. The heat exchanger length, is limited by the number of nodes in the academic version and the calculation power of the computer. A small number of nodes provides a poor precision, while a too much discretized space (large number of nodes) leads to a long simulation time required to reach a converged solution.

5.1. GEOMETRY (DESIGNMODELER)

As previously mentioned, the geometry of the heat exchanger consists of 7 tubes with one of them in the middle. The hot fluid flows through the shell and the cold fluid through the tubes.

In order to obtain the design of the heat exchanger, different sketches have been used, one in order to draw the inner diameter of the tube, and another to draw the outer diameter and the last one to draw the diameter of the shell. The nominal diameters implemented are (Sinnott, 2008):

- Inner diameter of tubes: 1.68 cm
- Outer diameter of tubes: 2 cm
- Diameter of the shell: 15 cm

Sketches are plot in the YZ Plane so that the fluid flows corresponds to the X axis positive direction. In order to reproduce the depth of the 3 sketches in 3D the Extrude tool is used in the Both – Symmetry direction of 10 cm and 20 cm respectively in order to have, in both directions (front and back) of the sketch the mentioned depth. This generates the 0.2 m and 0.4 m length of the heat exchanger, respectively.

Using the Extrude tool an Add Frozen has been executed for the shell, therefore an independent body is created, with separate faces and edges. For the sketches of the tubes it has been done a Slice Material to slice out resultant body (tubes) from the existing Frozen body and identify the presence of the tubes side independently of the shell side.

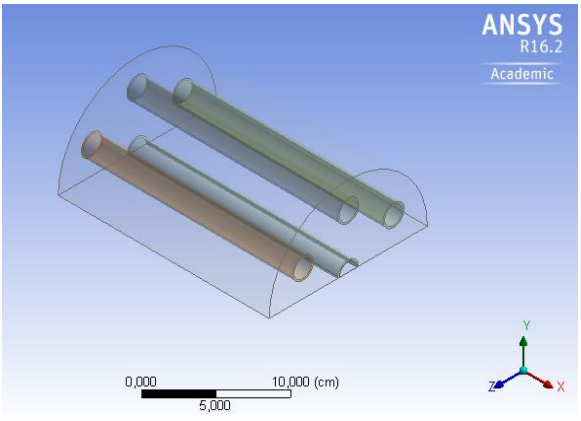

Figure 2. Heat exchanger of 0.2 m

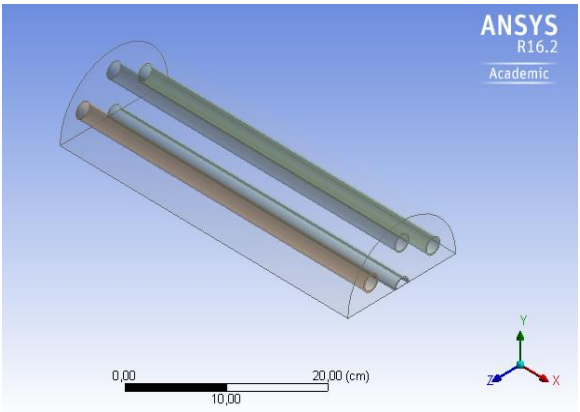

Figure 3. Heat exchanger of 0.4 m

5.1.1. Symmetry

The Symmetry tool has been used in order to obtain the design of only a half of the heat exchanger. In this way, ANSYS® will perform the simulation as if the whole heat exchanger was present but the symmetry provides the advantage of working only with half of the nodes, which saves also in computation effort. The plane where the Symmetry is applied is the ZX Plane.

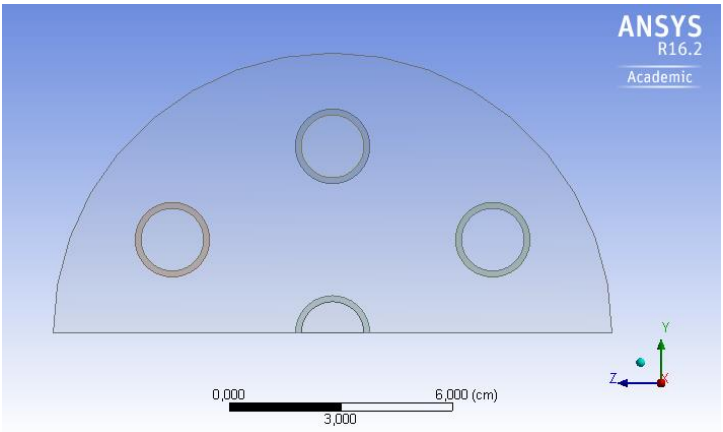

Figure 4. ZY Plane

5.2. MESHING

In this step, the geometry defined before is meshed. The default mesh controls of ANSYS® program generates a mesh that is already adequate for the model analyzed. Nevertheless, a more precise mesh is required where the changes are greater, i.e. for the tubes. In the shell a thinner mesh than the ANSYS® default but not as fine as the tube's mesh.

The parameters modified are:

- For the 0.2 m heat exchanger:

Display:

- Physics preference: CFD
- Solver preference: Fluent

Sizing:

- Use Advanced Size Function: On: Curvature
- Relevance Center: Fine
- Smoothing: High
- Min Size: $3.81 \cdot 10^{-5}$ m (Tubes)
- Max Size: $7.62 \cdot 10^{-3}$ m (Shell)

Based on the previously results for the 0.2 m heat exchanger:

Statistics:

- Nodes: 118,977
- Elements: 134,682

Aspect Ratio:

- Min: 1.0362
- Max: 11.645

- For the 0.4 m heat exchanger:

Sizing:

- Min Size: $6.33 \cdot 10^{-5}$ m (Tubes)
- Max Size: $1.26 \cdot 10^{-2}$ m (Shell)

Based on the previously results for the 0.4 m heat exchanger:

Statistics:

- Nodes: 204,422
- Elements: 240,319

Aspect Ratio:

- Min: 1.2094
- Max: 12.18

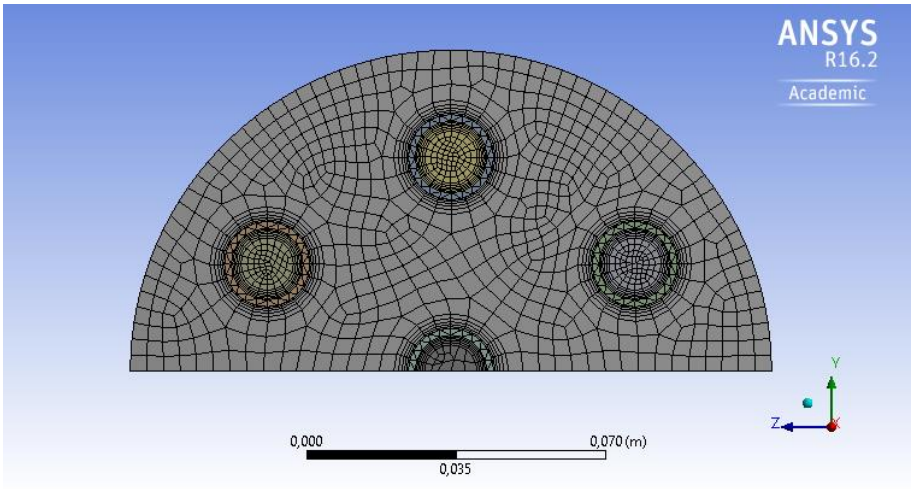

Figure 5. ZY Plane Mesh (L = 0.2 m)

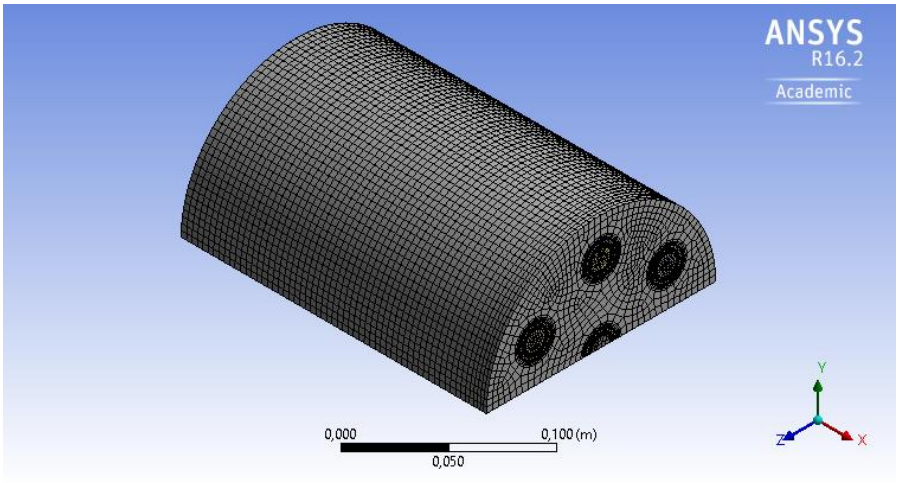

Figure 6. Isometric Plane Mesh (L = 0.2 m)

5.2.1. Inflation

To adequately resolve flow gradients near the wall a smaller mesh cells near the wall are required. An efficient way to achieve this is by inflating the wall surface mesh to produce layers of thin prismatic cells called inflation layers**.** Due to that, the inflation at the both tubes sides provides a more accurate heat transfer coefficients. By default 5 inflation layers in each side have been stablished.

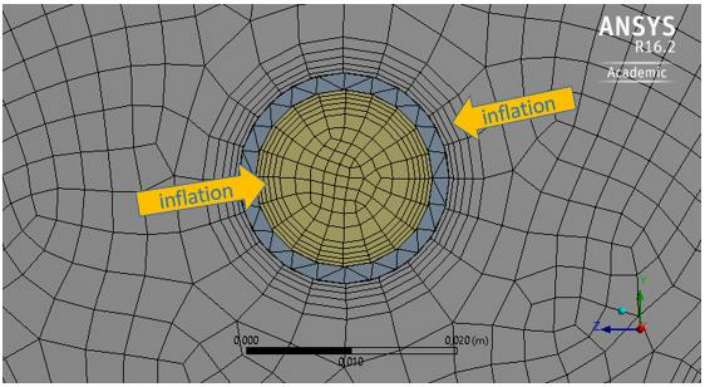

Figure 7. Inflation

5.3. BOUNDARY CONDITIONS

It is assumed that the heat exchanger tubes are made of copper and that the shell and tube fluids are both water. For the construction of the heat exchanger is required a weldable material (Perry, 2008). Table 1 provides the properties of copper and in the Table 2 are shown the properties of water.

Table 1. Properties of copper

Material Solid	**Copper (Cu)**
Density (kg/m^3)	8978
Cp (J/kg·K)	381
Thermal Conductivity (W/m·K)	387.6

Table 2. Properties of water

Material Fluid	**Water (H_2O)**
Density (kg/m^3)	998.2
Cp (J/kg·K)	4,182
Thermal Conductivity (W/m·K)	0.6
Viscosity (kg/m·s)	0.001003

5.3.1. Velocity Inlet

Velocity inlet boundary conditions are used to define the flow velocity. In this case the velocity inlet must be specified for both shell and tubes. A plug flow is assumed as an initial condition**.** Inside the shell, it is recommended that water does not flow below a velocity of 0.3 m/s. For the tubes it is recommended that water does not flow below 1.5 m/s (Sinnott, 2008). As it is discussed later, some simulations have been done with a velocity of 0.7 m/s also to make the results more graphically visible. In this section is where the initial temperature of the shell and tubes is selected too, this information is retrieved in Table 3.

5.3.2. Pressure Outlet

In this section has been set P = 0 at the exit of the shell and tubes. With this boundary condition ANSYS® processes that there is atmospheric pressure at the exit of the shell and tubes, for that reason ANSYS® calculates in each point the corresponding pressure from the inlet to the outlet where atmospheric pressure is meant to be.

5.3.3. Shell Wall

For the shell wall, the heat flux set towards the exterior is zero, so that ANSYS® process that walls of the shell as adiabatic.

5.3.4. Simulations

5.3.4.1. Simulations for a 0.2 m length heat exchanger

Inlet conditions for the shell and tubes are necessary to be established in order to evaluate the convective coefficients and the pressure drop of the heat exchanger. Temperature and velocity are defined in this step. Reynolds number is higher from 4,000 so the flow is fully turbulent. Table 3 and Table 4 shows the different inlet conditions for the heat exchanger base case (0.2 m length) and for the heat exchanger case (0.4 m length).

Table 3. Inlet conditions for a length of 0.2 m

Simulation	1	2	3	4
Type of Flow	Co-current	Counter-current	Co-current	Counter-current
Velocity (m/s)	0.7	0.7	1.5	1.5
T shell (ºC)	90	90	90	90
T tubes (ºC)	10	10	10	10
Reynolds shell	20342	20342	20342	20342
Reynolds tubes	11739	11739	25155	25155

5.3.4.2. Simulations for a 0.4 m length heat exchanger

Table 4. Inlet conditions for a length of 0.4 m

Simulation	**5**	**6**	**7**	**8**
Type of Flow	Co-current	Counter-current	Co-current	Counter-current
Velocity (m/s)	0.7	0.7	1.5	1.5
T shell (ºC)	90	90	90	90
T tubes (ºC)	10	10	10	10
Reynolds shell	20342	20342	20342	20342
Reynolds tubes	11739	11739	25155	25155

5.4. SOLVER

In order to make the simulations, the same type of Solver method has been used for all 8 case studies, the model used is the Standard k-ε as already mentioned in the section 3.2.2.1. Details of this Solver are the following:

- Turbulence Model: k-ε
- k-ε Model: Standard
- Near-Wall Treatment: Enhanced Wall Treatment
- Pressure-Velocity Coupling: Coupled
- Gradient: Least Squares Cell Based
- Pressure: Second Order
- Momentum: Second Order Upwind
- Turbulent Kinetic Energy: Second Order Upwind
- Turbulent Dissipation Rate: Second Order Upwind
- Energy: Second Order Upwind
- Precision: Double Precision

6. RESULTS

ANSYS® results are compared to the classical equations for the shell and tube heat exchanger. To apply the classical equations to obtain the convection coefficient and the pressure drop (equations available in section 3.1.1 and 3.1.2) an average of the temperatures values from the inlet to the outlet of the tube side and shell side have been considered for the fluid, an average of the temperatures values for the tubes walls have been considered too in order to calculate the fluid viscosity at the bulk fluid temperature and the fluid viscosity at the wall (Serth, 2007).

Eight scenarios have been simulated, half of them with 0.2 m and the other half with 0.4 m heat exchanger length. All the CFD equations (available in section 3.2.1 and 3.2.2) have converged according to the residuals values as described in section 3.3.4.

Post program visualization tools are used to get insights on the internal behavior: inside shell and tubes. The tubes are numbered for their identification, being the central tube the number 4 (Figure 8).

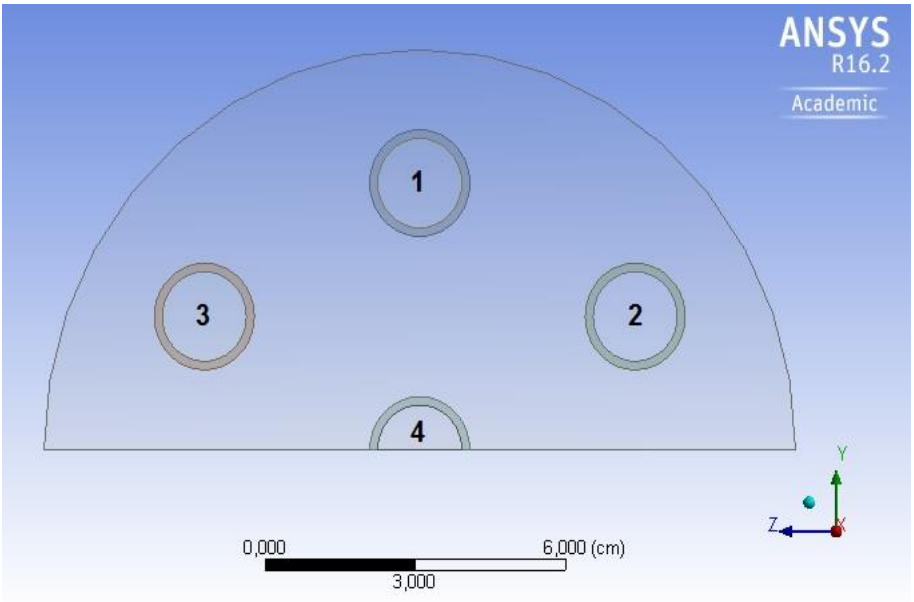

Figure 8. Exchanger sketch with the numbered tubes

6.1. Heat exchanger base case (0.2 m length)

6.1.1. Co-current with low velocity tubes side (1st Simulation)

Converged simulations are processed using the ANSYS® Post tool. The characteristics of the 1st simulation are presented in Table 3 in section 5.3.4.1. The results obtained from ANSYS® simulation and the results calculated with the classical equations are presented in Table 5 and the outlet temperatures are the following:

- T outlet shell (ºC): 89.0
- T outlet tubes 1, 2, 3 (ºC): 13.2
- T outlet tube 4 (ºC): 14.5

Table 5. Results and comparison for the 1st Simulation

1st Simulation	ANSYS®	CLASSICAL	Dif. (%)
h_s tubes 1,2,3 (W/m²·K)	3670	2230	39
h_s tube 4 (W/m²·K)	4137	2222	46
h_i tubes 1,2,3 (W/m²·K)	4553	3715	18
h_i tube 4 (W/m²·K)	5150	3713	28
ΔP_s (Pa)	9.1	11.9	31
ΔP_i (Pa)	136.9	102.7	25

The central tube number 4 has higher convection coefficients than the other surrounding tubes according to ANSYS® simulation (Table 5). Hence the central tube outlet temperature is higher than for the other tubes. The reason is that its central location confers a higher velocity gradient and turbulence than for the other tubes where the fluid is slow down in contact with the shell. The unit symmetry means that all the surrounding tubes have the same results. The classical equations do not take into account the tube location in the shell and all the tubes are equivalent.

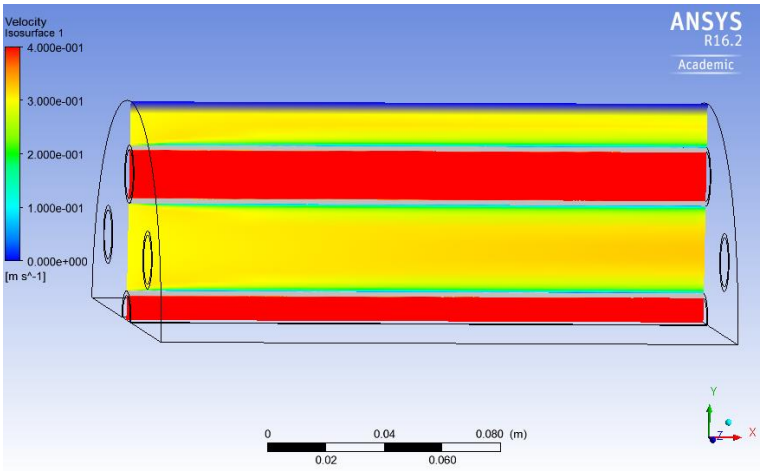

Figure 9. Velocity Isosurface XY Plane

The difference between ANSYS® results and the Classical results is consequence of the fact that the classical equations do not take into account the non-stabilized profiles while ANSYS® considers the microscopic balances in each point of the control volume. For the tube side convection coefficient, Eq. 3 in section 3.1.2 takes into account the non-stabilized profile, hence the difference between ANSYS® and classical equations is lower than for the shell side, where this term has not been developed.

Figure 10 shows the unstabilized profile of temperature for the 2nd and 3rd tube. A ZX Plane that cuts in the middle of the 2nd and the 3rd tube is created in order to visualize the evolution of the temperature along the tubes. The stablished range to visualize the variation of the temperature in the tubes is about 10 ºC and for that reason the shell is all above this temperature (red colour).

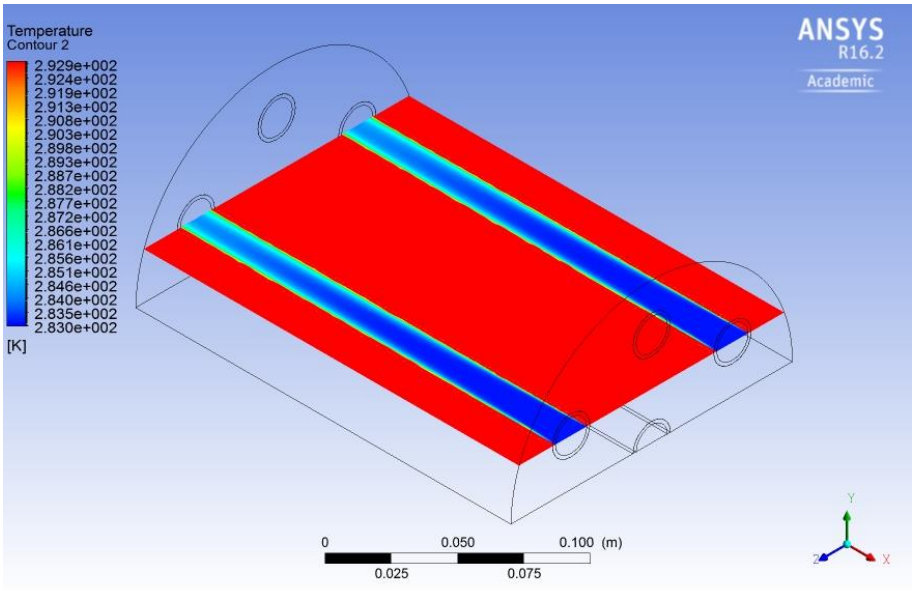

Figure 10. Isometric Temperature Contour 1st Simulation

Figure 11 shows the comparison between the ZX Plane presented in Figure 10 and the Symmetry Plane in order to visualize the difference between the middle tube and the rest of the tubes (2nd and 3rd ones, as represented here) as it has been noticed before, outlet temperature for 4th tube is higher.

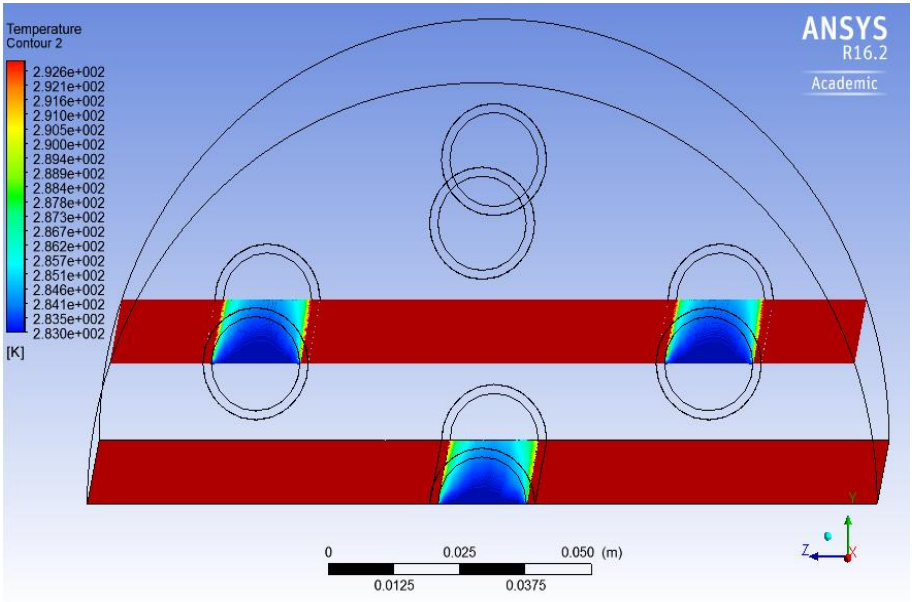

Figure 11. Temperature Contours 1st Simulation

Using the same ZX Plane, the unstabilized profile of velocity is clearly identified. In this case, all the tubes have the same velocity contour inside, also the 4th tube. Figure 12 shows the plug flow at the entrance and how it evolves along the tube while the fluid slows down near the walls and moves faster in the middle. The averaged velocity in a section is constant as the flow rate must be constant according to the overall mass balance. The fluid flowing inside the shell is also slowed down by the tubes outer walls.

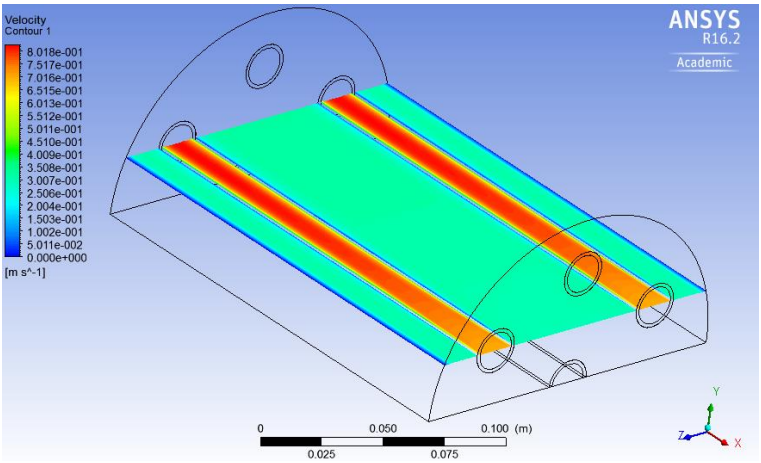

Figure 12. Isometric Velocity Contour 1st Simulation

Figure 13 represents the velocity profiles in vector form. In this case the simulation has been made in co-current as pointed by the arrows. The arrows are thicker where the fluid flows more intensely and thinner where the fluid flows slowly in accordance with last paragraph discussion.

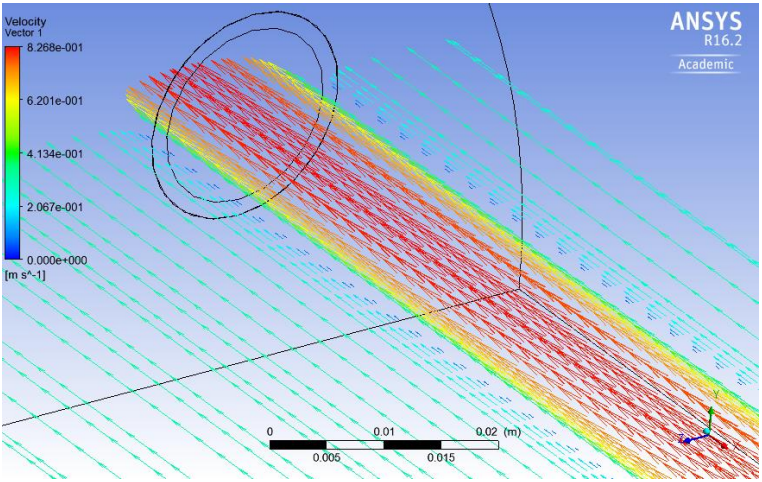

Figure 13. Velocity vectors 1st Simulation

The Figure 14 shows the pressure drop from the inlet to the outlet. Outlet pressure is zero and specified as boundary condition which means that at the outlet of the heat exchanger there is the atmospheric pressure. Pressure profiles are the same for all tubes, therefore using the ZX plane defined previously, pressure drop is observed for tubes 2 and 3. The highest pressure drop ΔP corresponds to the tubes, and very low ΔP in the shell, which is represented in blue color (Figure 14).

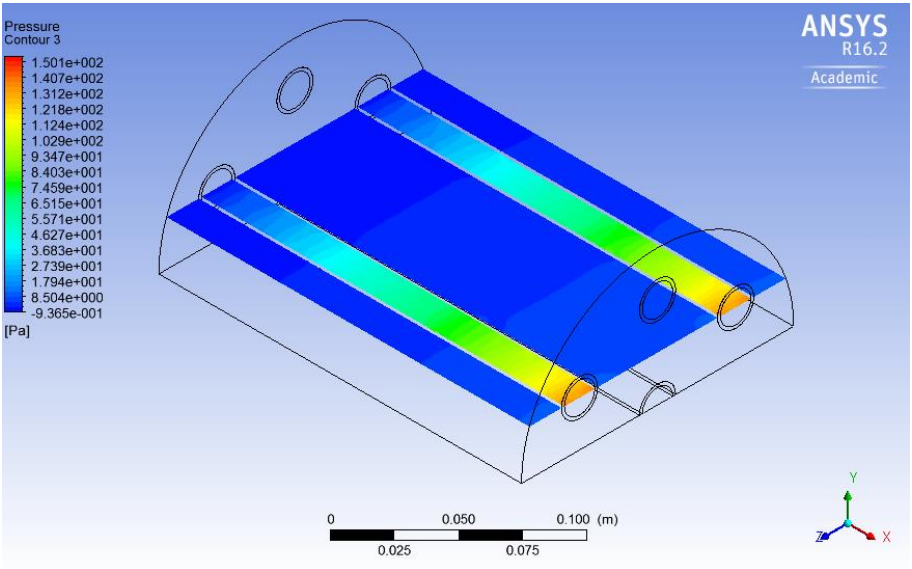

Figure 14. Isometric Pressure Contour 1st Simulation

The heat exchanger is made of 7 tubes and the shell, as described in section 5.1.1, although for ease of calculation effort, only half of it is plotted, taking advantage of the symmetry tool. Therefore, ANSYS® calculates as if the whole heat exchanger is present. In Figure 15 the entire heat exchanger is plotted in order to visualize the variation of pressure in all the tubes, while Figure 16 illustrates the entire heat exchanger covered by the shell to visualize the temperature contour.

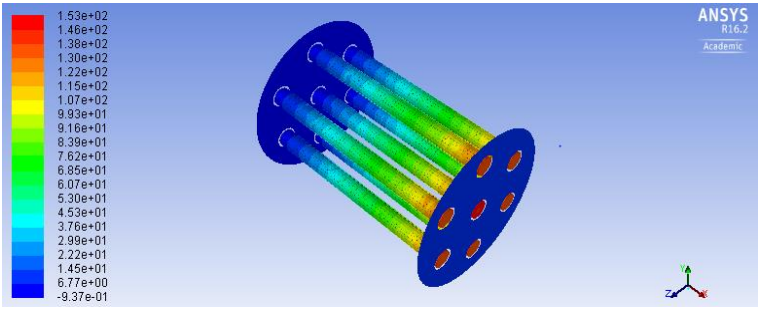

Figure 15. Pressure contour tubes from whole heat exchanger (Pa)

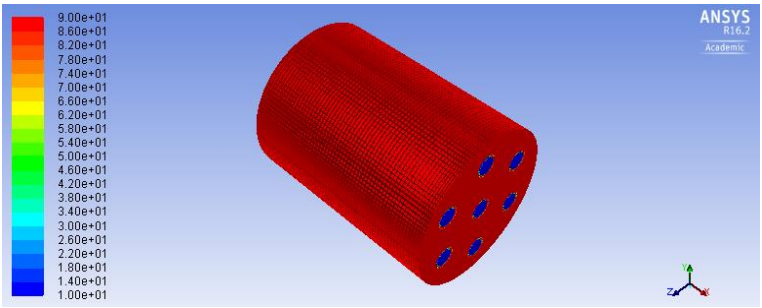

Figure 16. Temperature contour from whole heat exchanger (ºC)

6.1.2. Counter - Current with low velocity tubes side (2nd Simulation)

The characteristics of the 2nd simulation are presented in Table 3 in section 5.3.4.1. In this section is discussed the effect of operating the heat exchanger in counter-current instead of co-current as in the previous section (6.1.1).

The results obtained from ANSYS® simulation and the results calculated with the classical equations are presented in Table 6 and the outlet temperatures are the following:

- T outlet shell (ºC): 89.0
- T outlet tubes 1, 2, 3 (ºC): 13.6
- T outlet tube 4 (ºC): 15.1

Table 6. Results and comparison for the 2nd Simulation

2nd Simulation	ANSYS®	CLASSICAL	Dif. (%)
h_s tubes 1,2,3 (W/m²·K)	3720	2234	40
h_s tube 4 (W/m²·K)	4199	2237	47
h_i tubes 1,2,3 (W/m²·K)	4627	3733	19
h_i tube 4 (W/m²·K)	5233	3699	29
ΔP_s (Pa)	9.1	11.9	31
ΔP_i (Pa)	136.9	102.5	25

The same tendency observed in the 1st simulation is observed for the 2nd simulation. As far as the convection coefficients are concerned, the results from ANSYS® turned out to be higher than the ones calculated with the classical equations of chemical engineering handbooks. The pressures drops turned out to be the same ones obtained in the 1st Simulation because the only parameter that has been changed is the flow direction, in this case counter-current. It is also observed that the outlet temperature of tube 4 keeps being higher than the other tubes because it shows also higher convection coefficients.

In this 2nd simulation, the fluid flows through the tubes in counter-current, which results in a higher outlet temperature of the tubes and a slightly lower outlet temperature of the shell. The convection coefficients turn out to be higher compared with the co-current case with the same operating parameters. That is, is observed that indeed, working in a counter-current flow a higher efficiency is achieved. In the case of classical equations a very little variation in the coefficients and pressure drop is observed because temperature is only relevant for the calculus of viscosities.

Figure 17 shows the unstabilized profile of temperature in an Isometric Plane. A slight difference between Figure 10 can be observed due to the major efficiency of counter-current flow in terms of the outlet temperature.

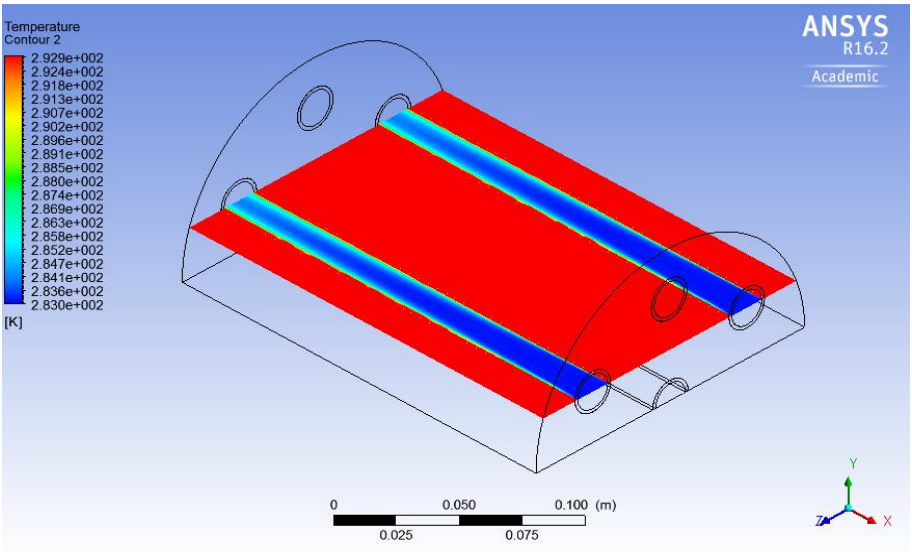

Figure 17. Isometric Temperature Contour 2nd Simulation

A comparison between the plane that cuts the 2nd and 3rd tube with the symmetry plane is realized in order to visualize the difference of temperatures in Figure 18.

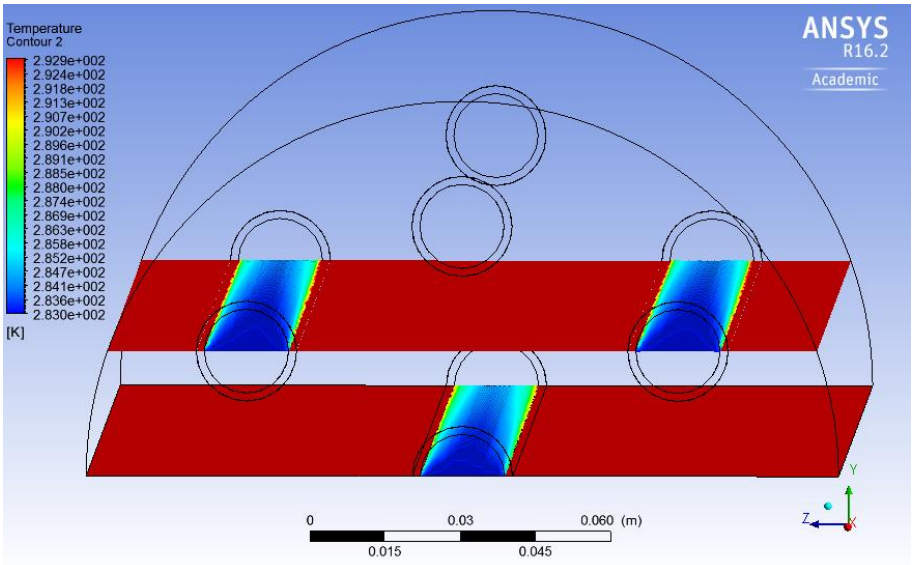

Figure 18. Temperature Contours 2nd Simulation

As far as the velocity is concerned, the plot is the same as the 1st simulation, as it has been mentioned, the only thing that has been varied is the side where the fluid enters in the tubes.

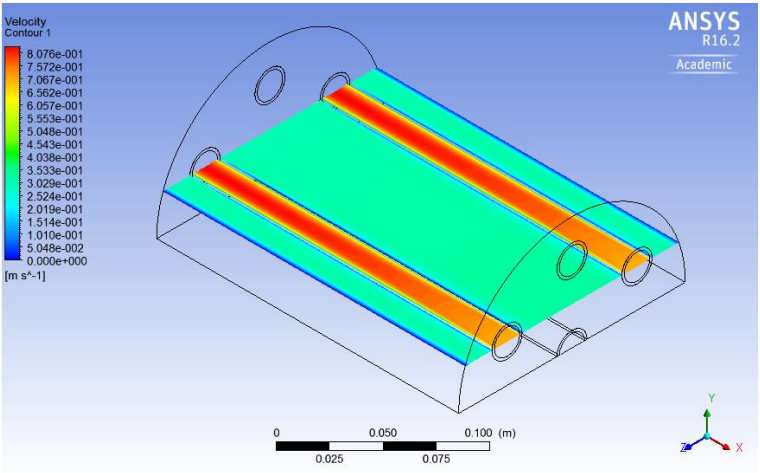

Figure 19. Velocity Contour 2nd Simulation

If velocity vectors are represented, it will be observed that the fluid of the shell flows in an opposite way to the fluid of the tubes because the arrows point out in an opposite direction.

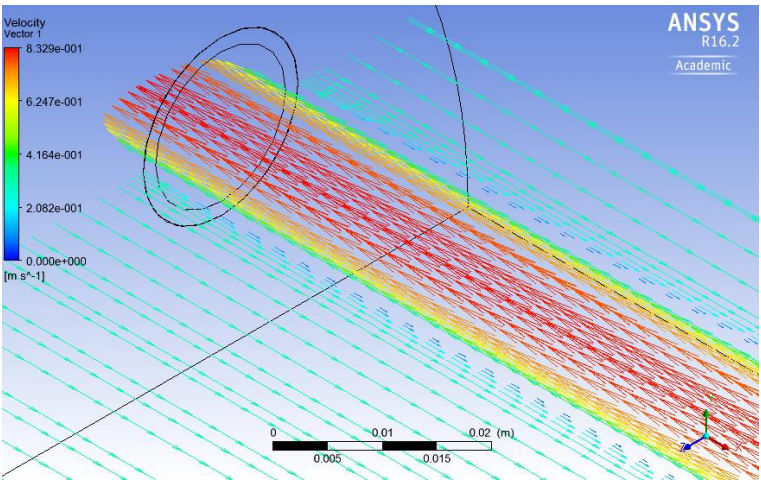

Figure 20. Velocity vectors 2nd Simulation

Figure 21 shows that the plot of the pressure evolution is the same as the 1st simulation.

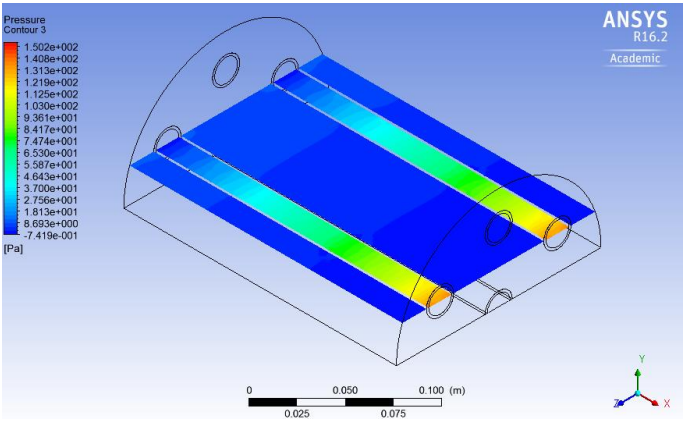

Figure 21. Pressure Contour 2nd Simulation

6.1.3. Co-Current with fast velocity tubes side (3rd Simulation)

The characteristics of the 3rd simulation are presented in Table 3 in section 5.3.4.1. The aim of the section is to study the effect of the flow rate inside the tubes.

For this 3rd simulation, the procedure is the same as the previous simulations:

- T outlet shell (ºC): 88.9
- T outlet tubes 1, 2, 3 (ºC): 12.0
- T outlet tube 4 (ºC): 15.0

Table 7. Results and comparison for the 3rd Simulation

3rd Simulation	ANSYS®	CLASSICAL	Dif. (%)
h_s tubes 1,2,3 (W/m²·K)	6673	2166	68
h_s tube 4 (W/m²·K)	7393	2168	71
h_i tubes 1,2,3 (W/m²·K)	8523	6657	22
h_i tube 4 (W/m²·K)	9484	6666	30
ΔP_s (Pa)	9.1	12.2	34
ΔP_i (Pa)	467.1	484.6	4

The main differences between classical and ANSYS have been already discussed in section 6.1.1 and this section focus on the effect of a flow rate increase inside the tubes. Comparing the convective coefficients of Table 5 and Table 6 from Table 7 it is stated that now they are higher than the other previous simulations due to the higher velocity in the tubes from 0.7 m/s to 1.5 m/s. In Table 7 there is a difference between the shell side coefficients of the classical equations and the ANSYS® ones. The classical equations consider only the shell side for the calculation of the shell side convective coefficients without considering the interaction with inside the tubes, which in turn are taken into account in ANSYS® software.

The pressure drop of the tubes has been increase compared with the 1st and 2nd simulation due to the higher velocity of the fluid.

Figure 22 shows the evolution of the temperature through the tubes in this 3rd simulation. As a consequence of the increase of velocity, the outlet temperature of tubes that surrounds the central tube are lower than in previous simulations due to the less time that the fluid is flowing inside the tubes even though the higher convective coefficients.

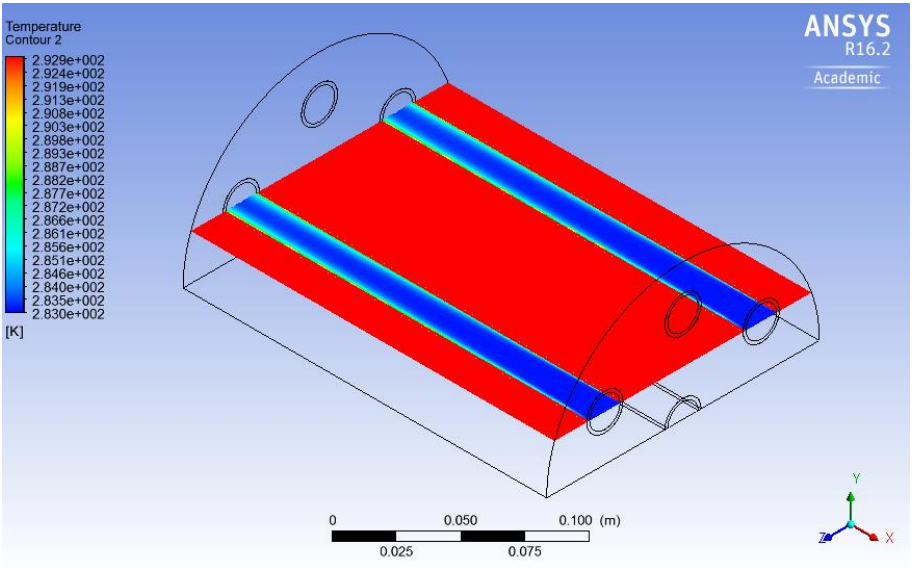

Figure 22. Temperature Contour 3rd Simulation

The central tube is 3ºC above the surrounding tubes, which difference is showed in Figure 23.

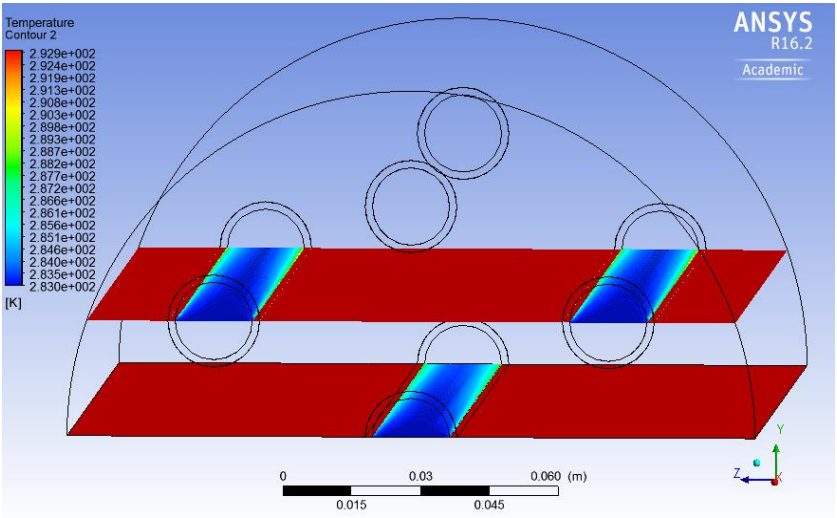

Figure 23. Temperature Contours 3rd Simulation

Velocity contours for the 3rd simulation are showed at Figure 24. It can be observed that the velocity of tubes is higher than in the shell. The range of the flow velocities has changed to a larger value so the color of the shell has also changed compared to the 1st and 2nd simulation.

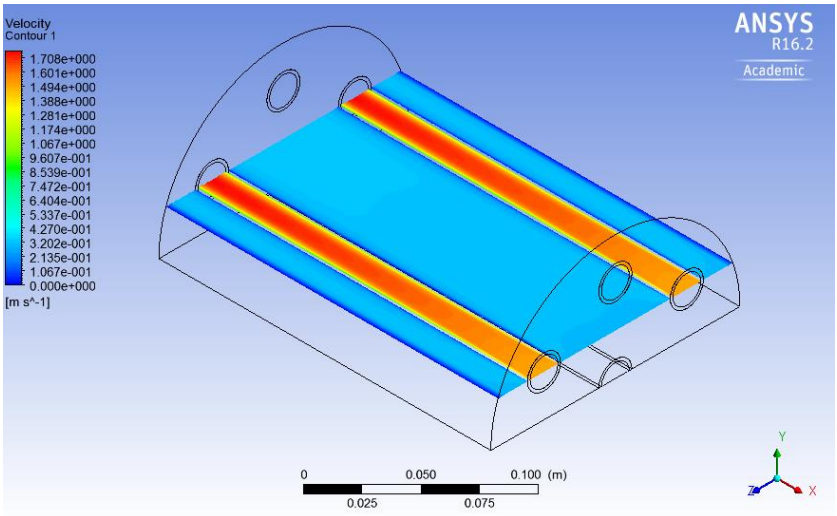

Figure 24. Velocity Contour 3rd Simulation

There is a significant variation with the pressure in the present simulation compared to the previous ones. The fact that the fluid flows in a higher velocity inside the tubes produces a higher pressure drop ΔP between the inlet and the outlet of all the tubes (Figure 25).

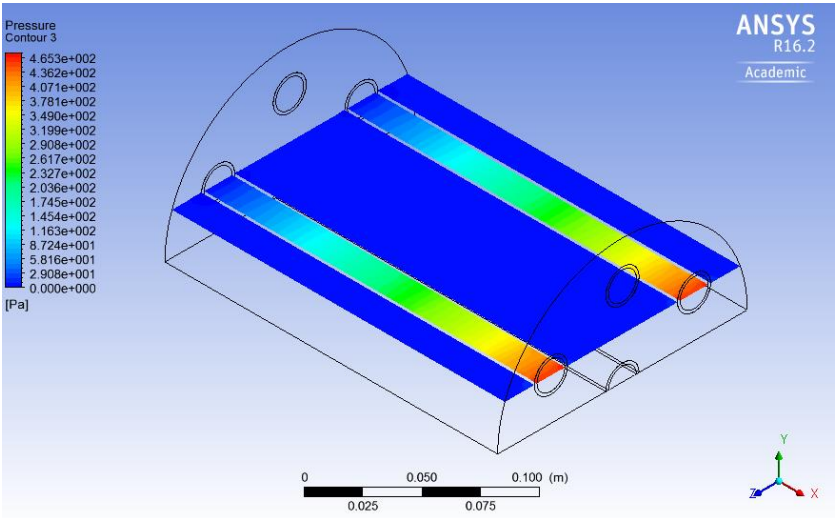

Figure 25. Pressure Contour 3rd Simulation

6.1.4. Counter-Current with fast velocity tubes side (4th Simulation)

The characteristics of the 4th simulation are presented in Table 3 in section 5.3.4.1. Finally, the effect of increasing the flow rate is also performed for the counter-current case. For this 4th simulation, the procedure is the same as the previous simulations:

- T outlet shell (ºC): 88.8
- T outlet tubes 1, 2, 3 (ºC): 12.2
- T outlet tube 4 (ºC): 15.1

Table 8. Results and comparison for the 4th Simulation

4th Simulation	ANSYS®	CLASSICAL	Dif. (%)
h_s tubes 1,2,3 (W/m²·K)	6777	2237	67
h_s tube 4 (W/m²·K)	7534	2162	71
h_i tubes 1,2,3 (W/m²·K)	8682	6727	23
h_i tube 4 (W/m²·K)	9678	6623	32
ΔP_s (Pa)	9.1	12.1	33
ΔP_i (Pa)	466.1	485.3	4

In the last simulation for the 0.2 m length heat exchanger, the same behavior as the previous simulations is appreciated. There is the difference between ANSYS® and the classical equations (discussed in section 6.1.1). The fact that operating in counter-current is more efficient than operating in co-current and also operating in counter-current flow has higher convection coefficients and outlet temperatures (discussed in section 6.2.2). The different convective coefficients between ANSYS® and the classical equations in the shell side when the velocity of the tubes is changed (discussed in section 6.3.3). No parameters have been modified so the pressure drop is still the same as the 3rd simulation.

An Isometric Plane is presented in Figure 26 to visualize the non-stabilized temperature profiles for the 4th simulation.

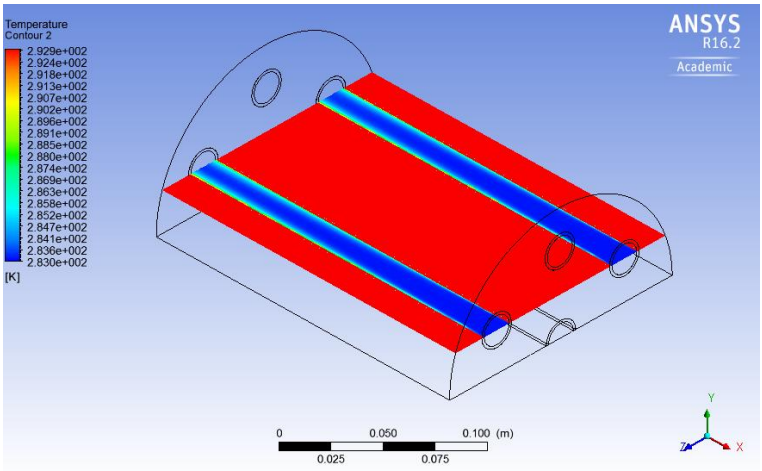

Figure 26. Temperature Contour 4th Simulation

The different outlets temperatures between the plane that cuts in the middle of the 2nd and the 3rd tube and the symmetry plane which contains the 4th tube is showed in Figure 27.

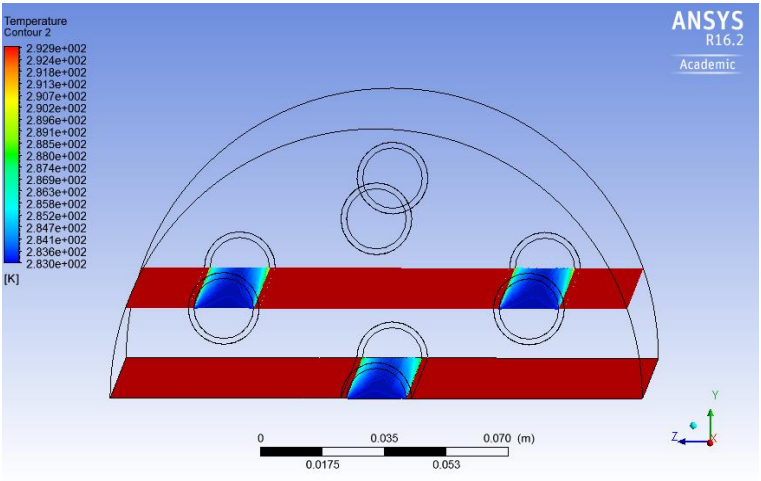

Figure 27. Temperature Contours 4th Simulation

The tube number 4 has no yellow colors at the outlet in their walls compared to the other tubes and it can be also observed that in tubes 2 and 3 at the middle of the tubes they have an intense blue color while tube number 4 not so much.

The velocity contour has been the same as the 3rd simulation as a consequence that no parameters have been modified.

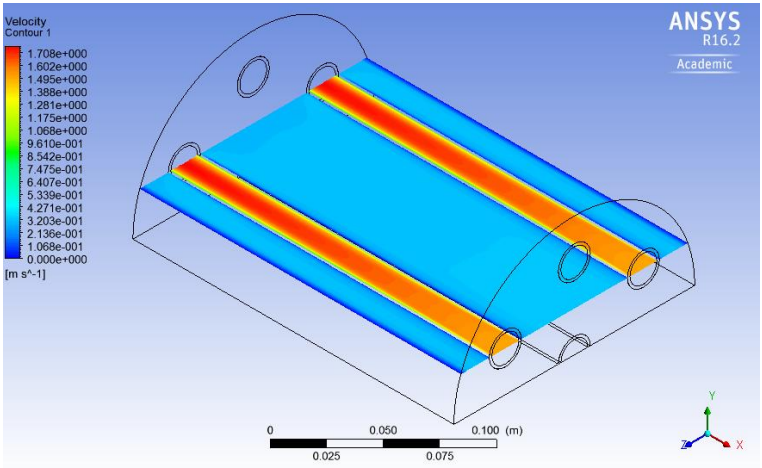

Figure 28. Velocity Contour 4th Simulation

A little variation is visualized in the pressure contour compared to the 3rd simulation in Figure 29. That is because the value of the legend has varied hence there is less red color in the inlet of the tubes, despite this the value for the pressure inlet and the pressure drop ΔP remains equal to the 3rd simulation.

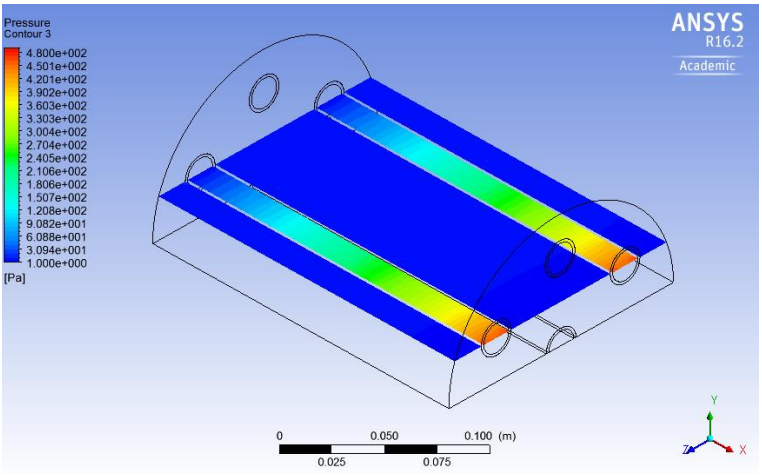

Figure 29. Pressure Contour 4th Simulation

6.2. Heat exchanger case (0.4 m length)

In this section the four simulations performed for the 0.2 m length heat exchanger base case are reproduced again with a 0.4 m heat exchanger to determine the effect of the heat exchanger length.

6.2.1. Co-current with low velocity tubes side (5th Simulation)

The characteristics of the 5th simulation are presented in Table 4 in section 5.3.4.2.

For this 5th simulation, the procedure is the same as the previous simulations but in a 0.4 m length heat exchanger:

- T outlet shell (°C): 88.5
- T outlet tubes 1, 2, 3 (°C): 15.8
- T outlet tube 4 (°C): 16.5

Table 9. Results and comparison for the 5th Simulation

5th Simulation	ANSYS®	CLASSICAL	Dif. (%)
h_s tubes 1,2,3 (W/m²·K)	3527	2228	37
h_s tube 4 (W/m²·K)	3887	2219	43
h_i tubes 1,2,3 (W/m²·K)	4360	3501	20
h_i tube 4 (W/m²·K)	4822	3485	28
ΔP_s (Pa)	15.1	23.7	57
ΔP_i (Pa)	248.8	209.5	16

Comparing the results obtained in that simulation from the 1st simulation, the conditions were the same with the difference of the length of the heat exchanger. The outlet temperatures are higher due to the major length of the heat exchanger. It can be observed that in that case, the convection coefficients are lower than the 1st simulation. In the classical method, the convection coefficients are lower due to the term of viscosities. The average of the temperatures is higher in the tube side and for that reason the convection coefficients get a lower value. In the shell side is practically the same value because the variation of temperature through the shell is very low. For the ANSYS® case with a 0.4 m length heat exchanger, the profiles are more stabilized than for the 0.2 m heat exchanger case. For that reason the velocity gradients are lower and the turbulence is lower. With a lower turbulence the value of the convection coefficients are lower too.

The pressure drop has been increased compared with the 1st simulation due to the major length of the heat exchanger. According to Bernoulli the length has been duplicate and the pressure drop in the tubes side for the ANSYS® and the classical case has been approximately duplicate too.

Figure 30 shows the variation of the temperature though the heat exchanger. A large difference compared with the 0.2 m heat exchanger is observed.

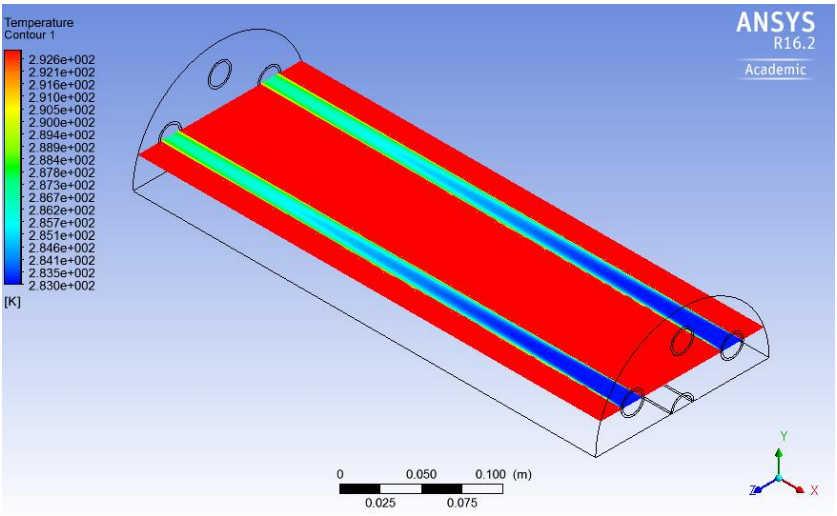

Figure 30. Temperature Contour 5th Simulation

The difference between the tubes number 2 and 3 with the tube number 4 is visualized in Figure 31.

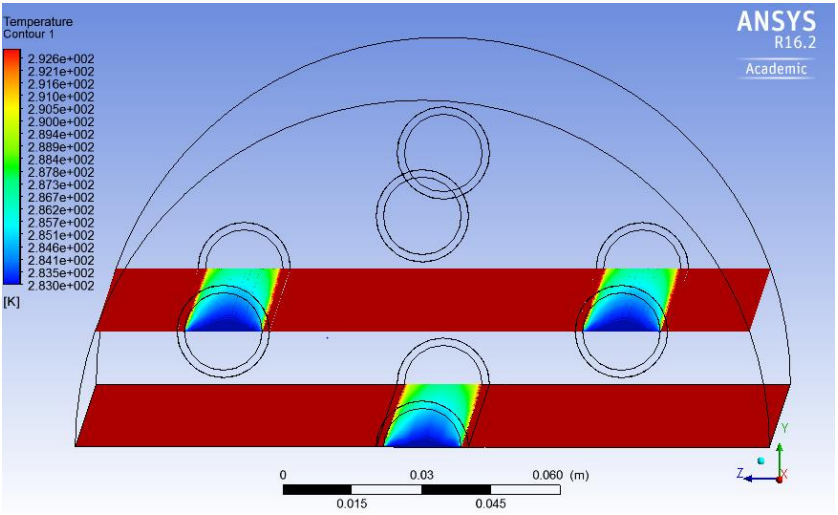

Figure 31. Temperature Contours 5th Simulation

Figure 32 shows the evolution of velocity inside the tubes.

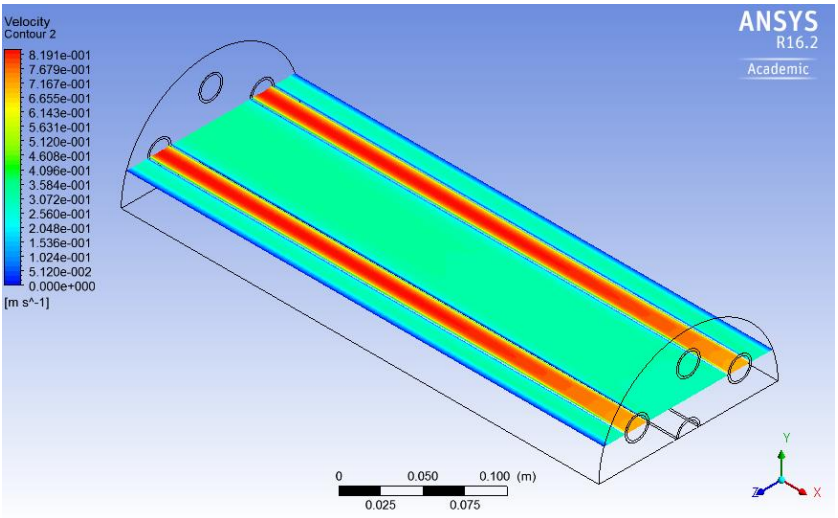

Figure 32. Velocity Contour 5th Simulation

Figure 33 illustrates the way the velocity is slowed down by the walls and how it increases at the center while the fluid is flowing through the tubes at the outlet of tubes with a better precision.

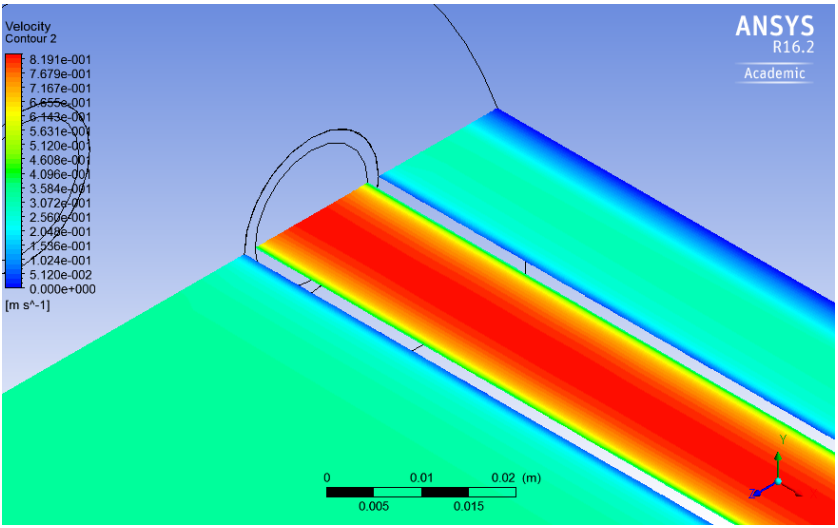

Figure 33. Velocity Outlet Contour 5th Simulation

Figure 34 allows to visualize the pressure drop from the inlet to the outlet of the tubes.

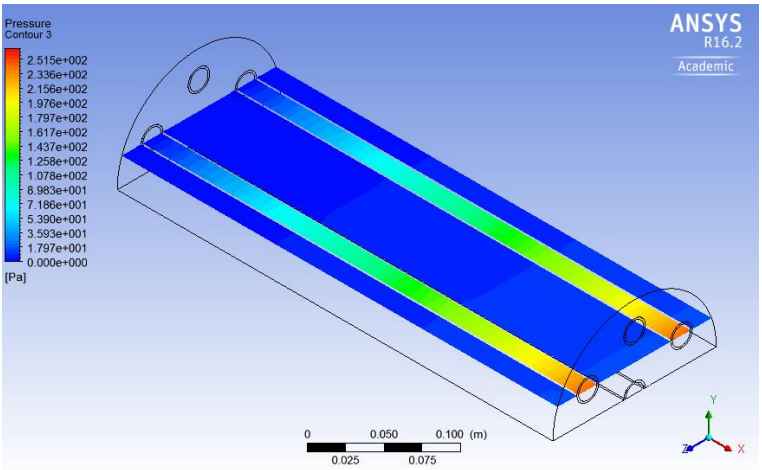

Figure 34. Pressure Contour 5th Simulation

6.2.2. Counter-current with low velocity tubes side (6th Simulation)

The characteristics of the 6th simulation are presented in Table 4 in section 5.3.4.2.

For this 6th simulation, the procedure is the same as the previous simulation:

- T outlet shell (ºC): 88.4
- T outlet tubes 1, 2, 3 (ºC): 16.1
- T outlet tube 4 (ºC): 16.8

Table 10. Results and comparison for the 6th Simulation

6th Simulation	ANSYS®	CLASSICAL	Dif. (%)
h_s tubes 1,2,3 (W/m²·K)	3577	2228	38
h_s tube 4 (W/m²·K)	3940	2224	44
h_i tubes 1,2,3 (W/m²·K)	4426	3515	21
h_i tube 4 (W/m²·K)	4893	3501	28
ΔP_s (Pa)	15.1	23.7	57
ΔP_i (Pa)	248.8	206.8	17

The results for that simulation keeps in the line discussed in detail in the previous sections. The values of the convective coefficients operating in counter-current are higher than the co-current due to the major efficiency in the 0.4 m heat exchanger case. Comparing the counter-current convective coefficients with the ones obtained in the 0.2 m heat exchanger they continue to have a lower value. The pressure drop values only have changed a few in the classical model due to the little variation of temperature in the viscosity term.

A little difference in the outlet temperature can be observed compared to the co-current 0.4 m case.

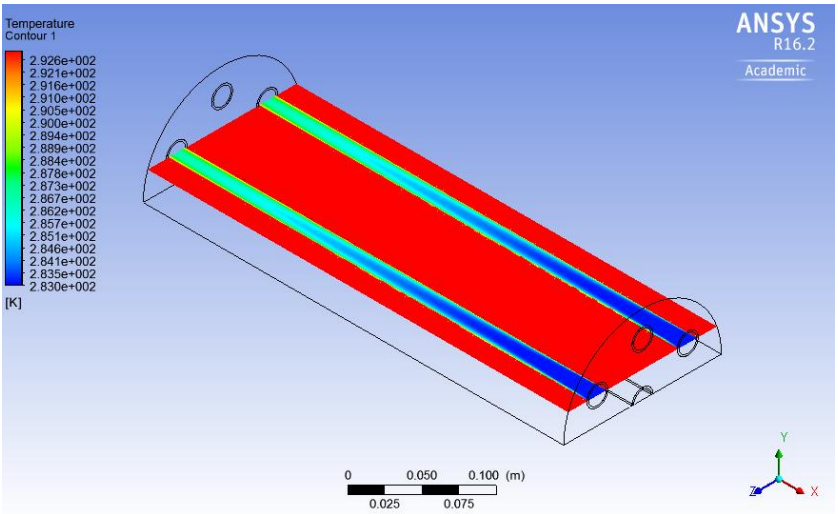

Figure 35. Temperature Contour 6th Simulation

Comparing the tube number 4 with tubes number 2 and 3, the difference is lower in terms of visualization because the difference is about 0.8 ºC. In a more detailed analysis a small difference can be observed in terms of colors defining the temperature inside the tubes (Figure 36).

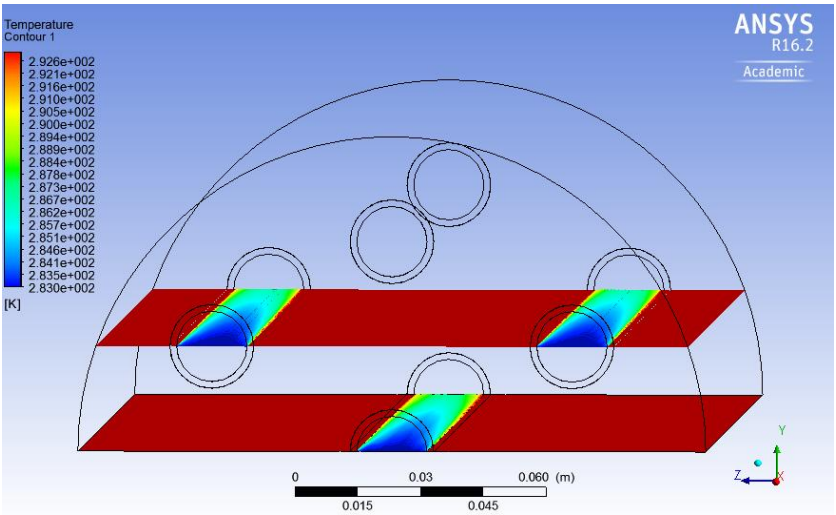

Figure 36. Temperature Contours 6th Simulation

The following figures illustrate that velocity and pressure maintain in the line as the previous simulations (Figure 37 and Figure 38, respectively).

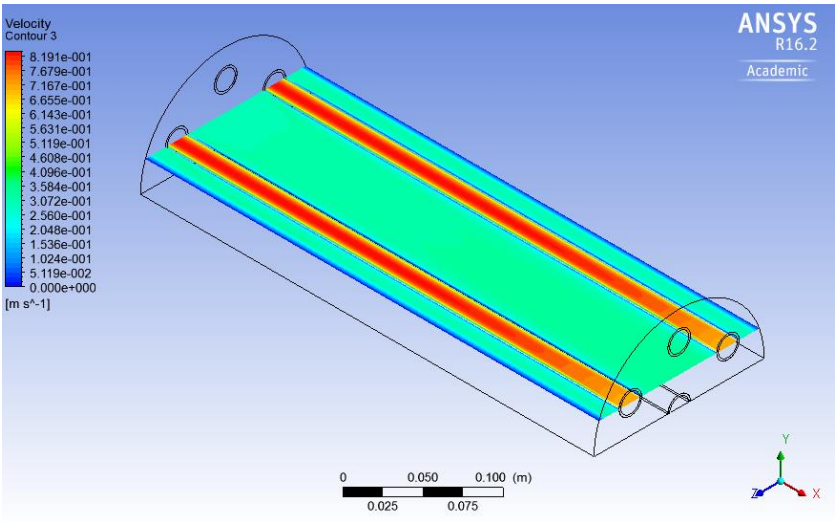

Figure 37. Velocity Contour 6th Simulation

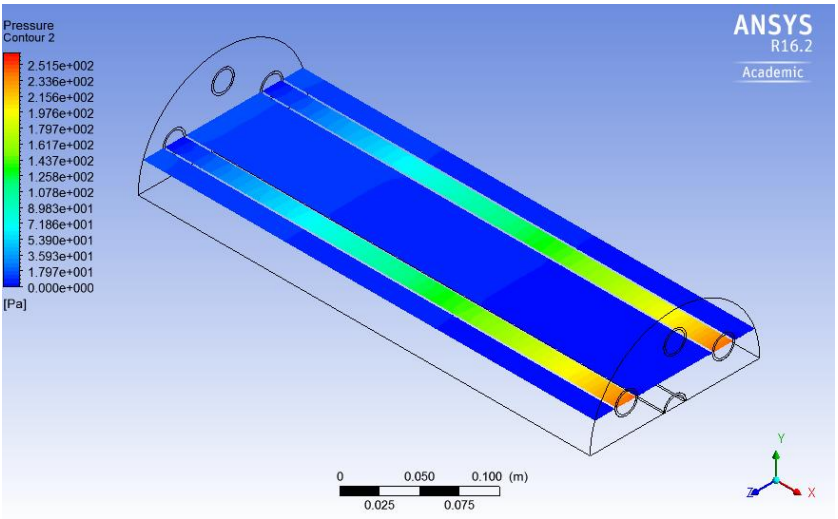

Figure 38. Pressure Contour 6th Simulation

6.2.3. Co-current with fast velocity tubes side (7th Simulation)

The characteristics of the 7th simulation are presented in Table 4 in section 5.3.4.2. For this 7th simulation, the procedure is the same as the previous simulation:

- T outlet shell (ºC): 88.0
- T outlet tubes 1, 2, 3 (ºC): 13.4
- T outlet tube 4 (ºC): 15.3

Table 11. Results and comparison for the 7th Simulation

7th Simulation	ANSYS®	CLASSICAL	Dif. (%)
h_s tubes 1,2,3 (W/m²·K)	6453	2170	66
h_s tube 4 (W/m²·K)	7010	2166	69
h_i tubes 1,2,3 (W/m²·K)	8192	6274	23
h_i tube 4 (W/m²·K)	8953	6241	30
ΔP_s (Pa)	15.1	23.6	56
ΔP_i (Pa)	849.6	945.2	11

The results for this simulation keeps in the line discussed in detail in the other previous sections.

Table 11 shows the results for the simulation. The rate inside the tubes is 1.5 m/s that provides a higher pressure drop together with the increase of the length of the heat exchanger. In the shell side all the parameters have been kept equal from all the simulations, only the length of the heat exchanger produces a bit higher pressure drop compared to the simulations of the 0.2 m heat exchanger.

The values for the outlet temperatures are lower than the 0.7 m/s co-current and counter-current cases in consequence of the less time the fluid is flowing inside the tubes.

Figure 39 can show this phenomena, the fluid is not heated as much as the other simulations for the 0.4 m heat exchanger.

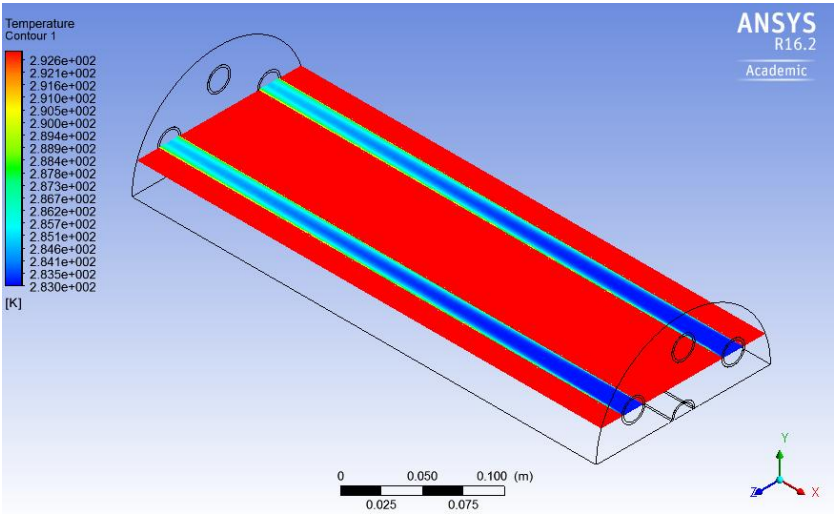

Figure 39. Temperature Contour 7th Simulation

The difference of about 2 ºC between the central tube and surrounding tubes is illustrated in Figure 40.

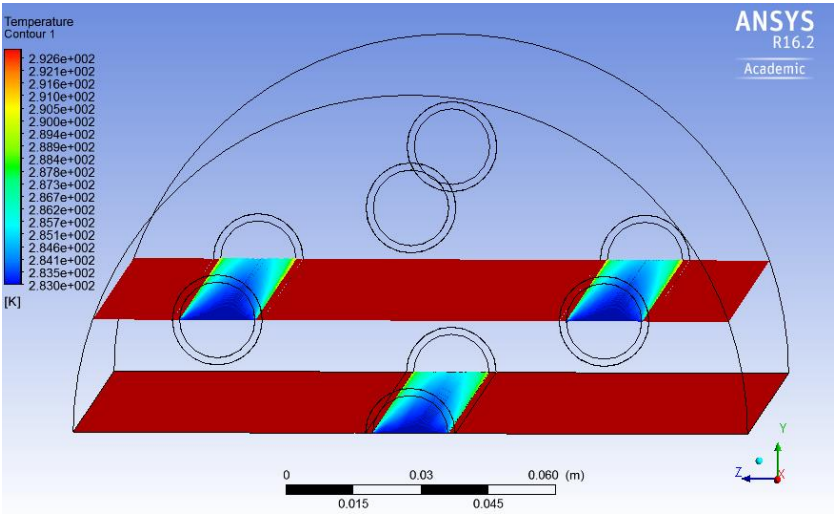

Figure 40. Temperature Contours 7th Simulation

Velocity contour is showed in Figure 41 with the same observations discussed in previous simulations.

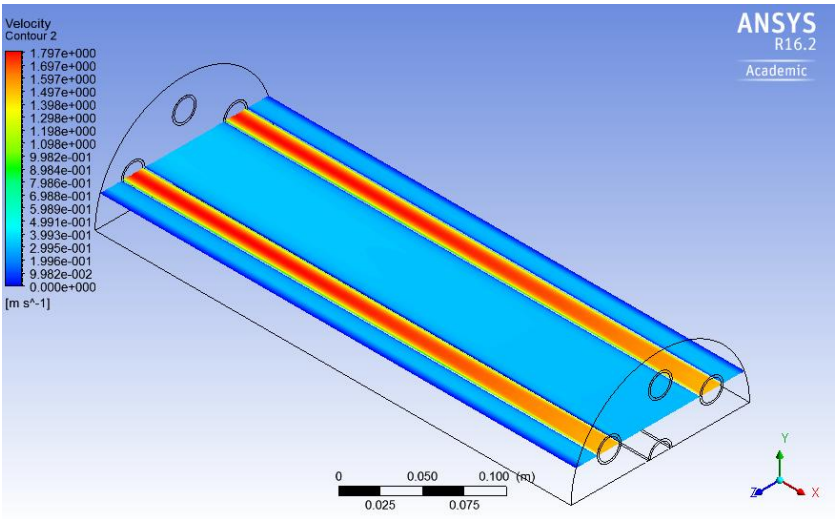

Figure 41. Velocity Contour 7th Simulation

There is a clear difference between all the simulations performed and this one in particular. The pressure drop has been the highest of all the simulations due to the velocity inside the tubes and the length of the heat exchanger. Figure 42 shows the values for the pressure from the inlet to the outlet.

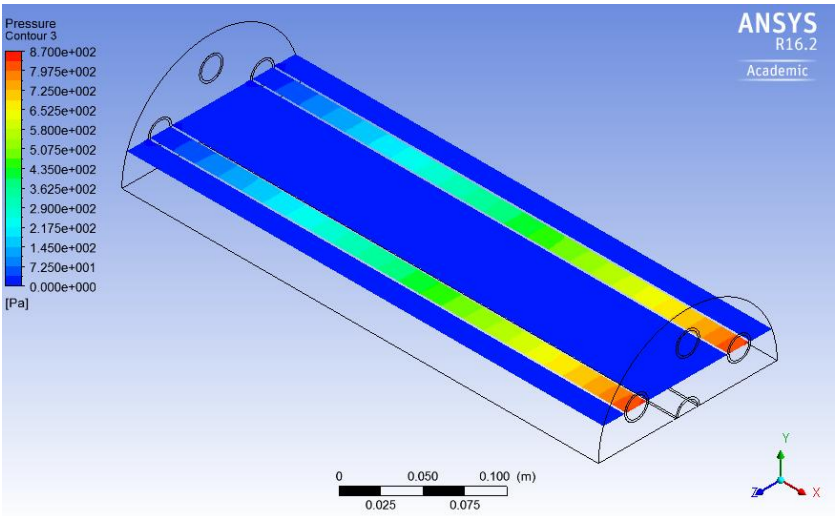

Figure 42. Pressure Contour 7th Simulation

6.2.4. Counter-Current with fast velocity tubes side (8th Simulation)

The characteristics of the 8th simulation are presented in Table 12 in section 5.3.4.2. For this 8th simulation, the procedure is the same as the previous simulation:

- T outlet shell (ºC): 87.9
- T outlet tubes 1, 2, 3 (ºC): 13.6
- T outlet tube 4 (ºC): 15.7

Table 12. Results and comparison for the 8th Simulation

8th Simulation	ANSYS®	CLASSICAL	Dif. (%)
h_s tubes 1,2,3 (W/m²·K)	6559	2224	66
h_s tube 4 (W/m²·K)	7125	2159	70
h_i tubes 1,2,3 (W/m²·K)	8347	6441	23
h_i tube 4 (W/m²·K)	9114	6241	32
ΔP_s (Pa)	15.1	24.4	62
ΔP_i (Pa)	849.6	942.5	11

The results for this simulation keep in the line discussed in detail in the other previous sections.

For this counter-current case the convection coefficients keep being higher than for the co-current case. The outlet temperatures are higher too in the tube side compared to the co-current case and the outlet temperature of shell keeps being lower. The pressure drop is the same as the previous simulation due to the velocity at which the fluid flows inside the tubes has been also 1.5 m/s. Figure 43 shows an Isometric Plane in order to visualize clearly the variation of the temperature in the tubes number 2 and 3.

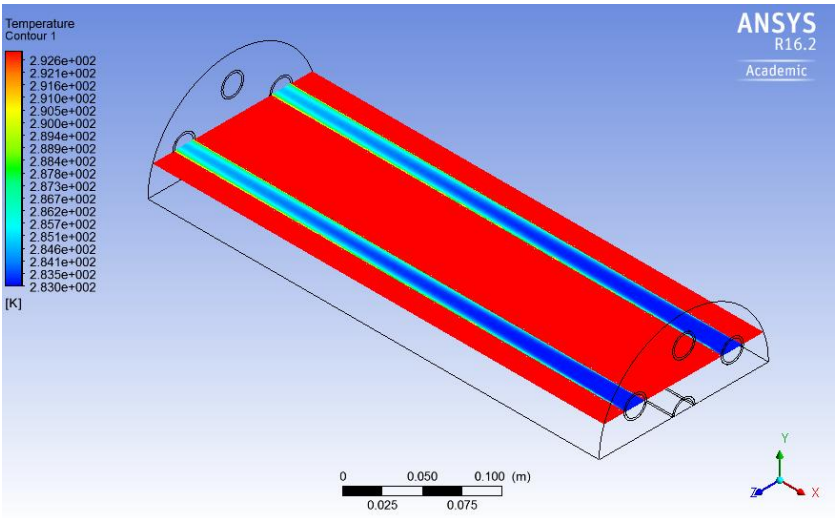

Figure 43. Temperature Contour 8th Simulation

The different evolution of the temperatures for tubes number 2 and 3 compared with the tube number 4 is presented in Figure 44 in a contour plot to visualize the variation of the colors.

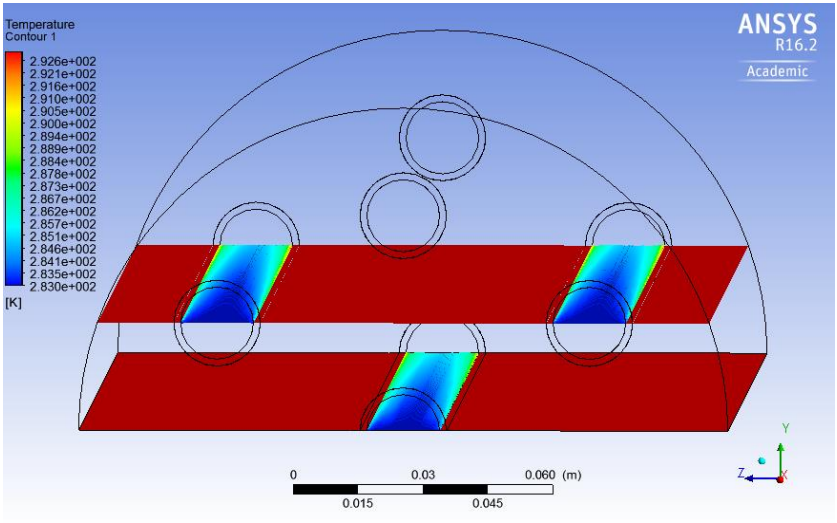

Figure 44. Temperature Contours 8th Simulation

Velocity contour is showed in Figure 45 with the same observations discussed in previous simulations.

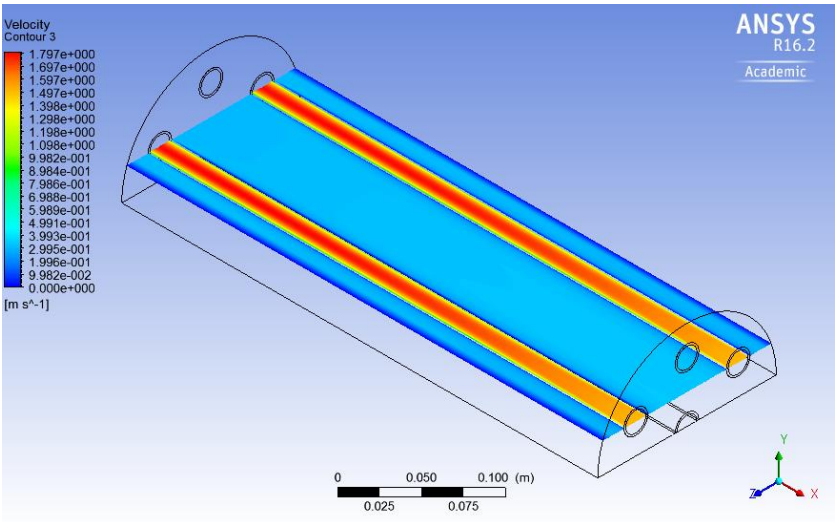

Figure 45. Velocity Contour 8th Simulation

Figure 46 shows the values for the pressure from the inlet to the outlet.

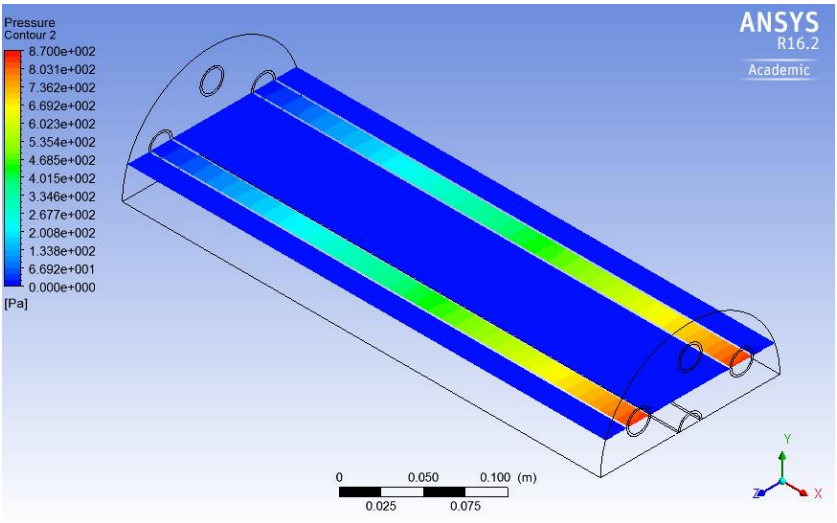

Figure 46. Pressure Contour 8th Simulation

7. CONCLUSIONS

- ANSYS® software allows to have a virtual laboratory able to save experimental laboratory time. The results have a rather good precision and parameters are easily assessed.
- ANSYS® takes into account the non-stabilized profiles while the majority of classical equations are only developed for the stabilized conditions.
- ANSYS® takes into account the interaction between the shell side and the tubes side for the convection coefficients. Without changing any parameter for the shell side, the convection coefficients have increased also in the shell side when the flow rate inside the tubes increases. The classical equations calculate the convection coefficients for the shell independently of the tubes.
- It can be observed that effectively operating in counter-current is more efficient than operating in co-current.
- ANSYS® takes into account the position of tubes inside the shell and how the turbulence can affect the convection coefficients. This aspect is not considered in classical equations.
- Working with ANSYS® a numeric visualization at microscopic level is provided with the Post-Processing program once the solution of the balances has been converged. Different contour plots such as temperature, velocity and pressure are represented for the shell and tube heat exchanger.

8. REFERENCES AND NOTES

ANSYS® Fluent 16.2 in Workbench User's Guide. ANSYS, Inc. License Manager Release 16.2, **2016**

ANSYS® Meshing User's Guide. ANSYS, Inc. License Manager Release 16.2, **2016**

ANSYS® Fluent Theory Guide. ANSYS, Inc. License Manager Release 16.2, **2016**

Alimoradi, A.; Veysi F. Prediction of heat transfer coefficients of shell and coiled tube heat exchangers using numerical method and experimental validation. International Journal of Thermal Sciences. **2016**, 107, 196 – 208

Dong, Q.W.; Wang, Y.Q.; Liu, M.S. Numerical and experimental investigation of shell side characteristics for RODbaffle heat exchanger. Applied Thermal Engineering. **2007**, 28, 651 - 660

Levenspiel, O. Flujo de fluidos e intercambio de calor. Barcelona: Reverté. **1993**

Llorens, J. Apunts de Fenòmens de Transport. Universitat de Barcelona. **2016**

Pal, E.; Kumar, I.; Joshi, J.B.; Maheshwari, N.K. CFD Simulations of shell side flow in a shell and tube type heat exchanger with and without baffles. Chemical Engineering Science. **2016**, 143, 314 - 340

Perry, R.H.; Green, D.W. Perry's Chemical Engineers' Handbook, 8th Edition. McGraw-Hill: United States of America. **2008**

Serth, R.W. Process heat transfer, principles and applications. 1st Edition. Burlington: Elsevier. **2007**

Sinnott, R.K. Chemical Engineering Design. 4th Edition. Burlington: Elsevier. **2008**, 6

Wen, J.; Yang, H.; Jian, G.; Tong, X.; Li, K.; Wang, S. Energy and cost optimization of shell and tube heat exchanger with helical baffles using Kriging metamodel base don MOGA. International Journal of Heat and Mass Transfer. **2016**, 98, 29 - 39

Zhang, M.; Meng, F.; Geng, Z. CFD simulation on shell and tube heat exchangers with small angle helical baffles. Chemical Science Engineering. **2015**, 9(2), 183 – 193

Zhou, G.; Xiao, J.; Zhu, L.; Wang, J.; Tu, S. A numerical study on the shell side turbulent heat transfer enhancement of shell and tube heat exchanger with trefoil-hole baffles. 7th International Conference on Applied Energy. **2015**, 75, 3174 - 3179

9. ACRONYMS

Nu → Nusselt number

h_s → Convection coefficient for the shell side (W/m²·K)

d_e → Equivalent diameter (m)

k_f → Fluid thermal conductivity (W/m·K)

j_h → Heat transfer factor

Re → Reynolds number

Pr → Prandtl number

μ → Fluid viscosity at the bulk fluid temperature (Pa·s)

μ_w → Fluid viscosity at the wall (Pa·s)

ΔP_s → Pressure drop for the shell side (Pa)

j_f → Friction factor

D_s → Shell diameter (m)

L → Tube length (m)

l_B → Baffle spacing (m)

ρ → Density (kg/m³)

u_s → Fluid velocity of the shell side (m/s)

u_t → Fluid velocity of the tube side (m/s)

h_i → Convection coefficient for the tube side (W/m²·K)

ΔP_i → Pressure drop for the tube side (Pa)

d_i → Inlet diameter (m)

$\vec{u}$ → The velocity vector (m/s)

E → The total energy per unit mass (J)

P → The static pressure (Pa)

J_j → Flux mass (kg/s)

$\vec{g}$ → Gravitational force (N)

$\bar{\bar{\tau}}$ → The stress tensor

$\vec{F}$ → External body forces (N)

I → The unit tensor (matrix identity)

k → Turbulence kinetic energy (J/kg)

ε → Turbulence dissipation rate (J/kg·s)

T → Temperature (ºC)

σ_ε → Turbulent Prandtl number for ε

σ_k → Turbulent Prandtl number for k